

Synthesis of β -Pyrrolic-Modified Porphyrins and Their Incorporation into DNA

Adam W. I. Stephenson,^[a] Ashton C. Partridge,^[a, b] and Vyacheslav V. Filichev^{*[a]}

Abstract: A synthetic methodology for the synthesis of various β -pyrrolic-functionalised porphyrins and their covalent attachment to 2'-deoxyuridine and DNA is described. Palladium(0)-catalysed Sonogashira and copper(I)-catalysed Huisgen 1,3-dipolar cycloaddition reactions were used to insert porphyrins into the structure of 2'-deoxyuridine and DNA. Insertion of a porphyrin into the middle of single-stranded CT oligonucleotides possessing a 5'-terminal run of four cytosines was shown to trigger the formation of pH- and

temperature-dependent i-motif structures. Porphyrin insertion also led to the aggregation of single-stranded purine-pyrimidine sequences, which could be dissociated by heating at 90 °C for 5 min. Parallel triplexes and anti-parallel duplexes were formed in the presence of the appropriate complementary strand(s). Depending on

Keywords: click chemistry • cycloaddition • DNA • porphyrinoids • thermal stability

the modification, porphyrins were placed in the major and minor grooves of duplexes and were used as bulged intercalating insertions in duplexes and triplexes. In general, the thermal stabilisation of parallel triplexes possessing porphyrin-modified triplex-forming oligonucleotide (TFO) strands was observed, whereas anti-parallel duplexes were destabilised. These results are compared and discussed on the basis of the results of molecular modelling calculations.

Introduction

DNA is an attractive supramolecular scaffold for the production of functionalised arrays due to its favourable characteristics such as its ability to functionalise DNA building blocks at will, the spontaneous self-assembly of complementary strands and the formation of helices as well as 2D and 3D structures.^[1] It can be recognised by proteins and other nucleic acid binding compounds. The covalent labelling of DNA, which results in modified oligonucleotides (ONs), can take place through the phosphate backbone, the nucleobase or the ribose sugar, locating the desired molecule in various positions around the DNA double helix, which allows for the production of controlled helical arrays. Porphyrins are useful labels and have been widely studied in a variety of applications including in light-harvesting devices^[2] and the production of reactive oxygen species.^[3]

The site-specific covalent attachment of porphyrin moieties to DNA has been achieved by using a variety of methodologies including the modification of nucleobases,^[4–9] ribo-

furanose residues,^[10–15] the phosphate backbone^[16,17] and acyclic linkers.^[18,19] Porphyrin moieties have been introduced as 3'- or 5'-molecular caps,^[13,19–21] as a nucleobase substituent in the middle of the helix^[18] or as a label in the minor^[11,17,22] and major^[5–9] grooves. Several tethers have been used for the covalent attachment of porphyrins including maleimidothiols,^[8,17] amides,^[11–13,15] phosphates^[16] and alkynes.^[4–7,9] The incorporation of the porphyrins as 5' and 3' caps has been shown to improve base-pair fidelity and duplex stability^[10] as well as showing the ability for the porphyrins to electronically communicate with each other (exciton coupling). This feature enables porphyrins to be used as detectors of DNA secondary structures in circular dichroism (CD) spectroscopy.^[12–16,21] The internal modification of ONs with porphyrins has recently become of interest for the development of helical scaffolds. Such examples include the synthesis of a DNA containing 11 *meso*-functionalised porphyrins on a single strand^[5,6] and a zipper porphyrin assembly in the major groove of a DNA duplex.^[7]

In contrast to the common functionalisation of a porphyrin at the *meso* position,^[5–9,11,20] which results in a system nearly orthogonal to the porphyrin core, we have recently synthesised a β -pyrrolic-modified porphyrin and shown that its H-aggregate formation in the minor groove significantly stabilised duplexes (ΔT_m per modification = +7.5–7.9 °C).^[22] Duplex thermal stability exceeded 90 °C when four porphyrins were stacked in the zipper motif as a result of superior interactions between β -pyrrolic-modified porphyrins in comparison with previously studied DNA-porphyrin constructs.^[5–8,17] We were curious, therefore, as to the effect of different attachments of β -pyrrolic porphyrin to DNA on

[a] Dr. A. W. I. Stephenson, Prof. A. C. Partridge, Dr. V. V. Filichev
College of Sciences, Institute of Fundamental Sciences
Massey University, Private Bag 11-222
Palmerston North (New Zealand)
Fax: (+64)6-350-5682
E-mail: v.filichev@massey.ac.nz

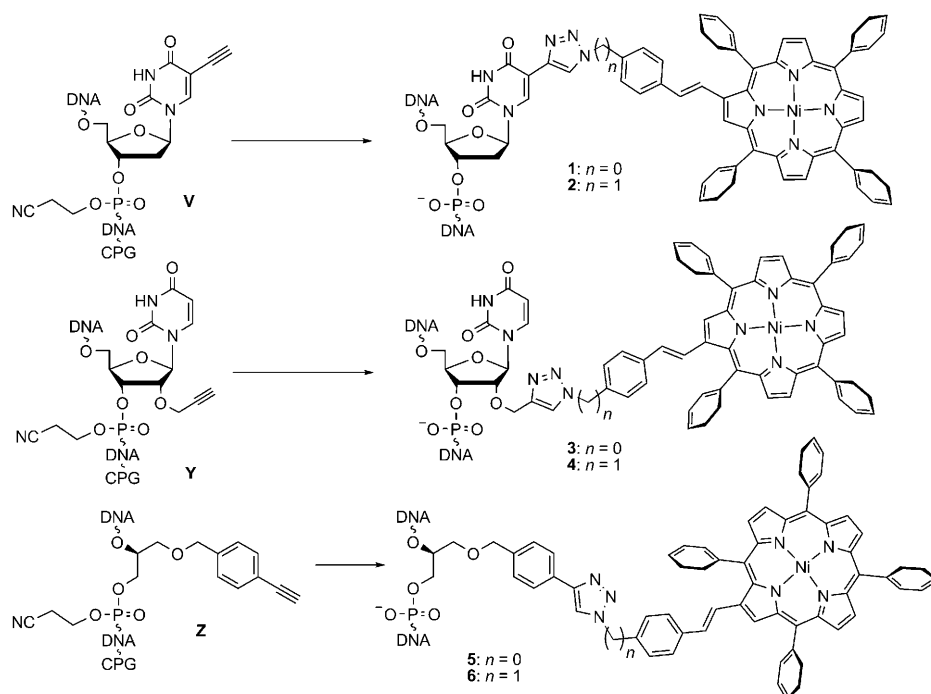
[b] Prof. A. C. Partridge
Present address: Auckland University, 20 Symonds Street
Auckland (New Zealand)

Supporting information for this article is available on the WWW under <http://dx.doi.org/10.1002/chem.201003200>.

binding affinity and the spectroscopic properties of DNA–porphyrin conjugates.

In this manuscript we report the synthesis of β -pyrrolic-functionalised porphyrins covalently attached to uridines using Sonogashira or copper(I) azide/alkyne cycloaddition (CuAAC)^[23] reactions. To screen the effect of different porphyrin locations in DNA duplexes, we preferred a post-synthetic modification of DNA^[24] using CuAAC in which a functional group of the label (azide) reacts with the complementary functional group on the DNA (terminal alkyne).^[25] This approach is more convenient than the time-consuming preparation of individual phosphoramidites especially taking into account the limited lifetime of porphyrin-containing phosphoramidites.^[11,12]

We prepared ONs possessing insertions of 2'-deoxy-5-ethynyluridine^[26] (**V**; Scheme 1), 2'-*O*-propargyluridine^[27] (**Y**) or (*R*)-4-ethynylphenylmethylglycerol^[28] (**Z**) and used



Scheme 1. Structures of porphyrin-functionalised ONs produced by CuAAC.

aromatic ($n=0$) or aliphatic ($n=1$) azidoporphyrins in subsequent conjugation reactions. This allowed the placement of porphyrins in major (**1** and **2**) and minor grooves (**3** and **4**) of the duplex as well as the use of porphyrins as intercalating bulged insertions in duplexes and triplexes (**5** and **6**). Thermal stability and circular dichroism studies were undertaken to assess the effect of each porphyrin modification on single-stranded, duplex and triplex DNA.

Results and Discussion

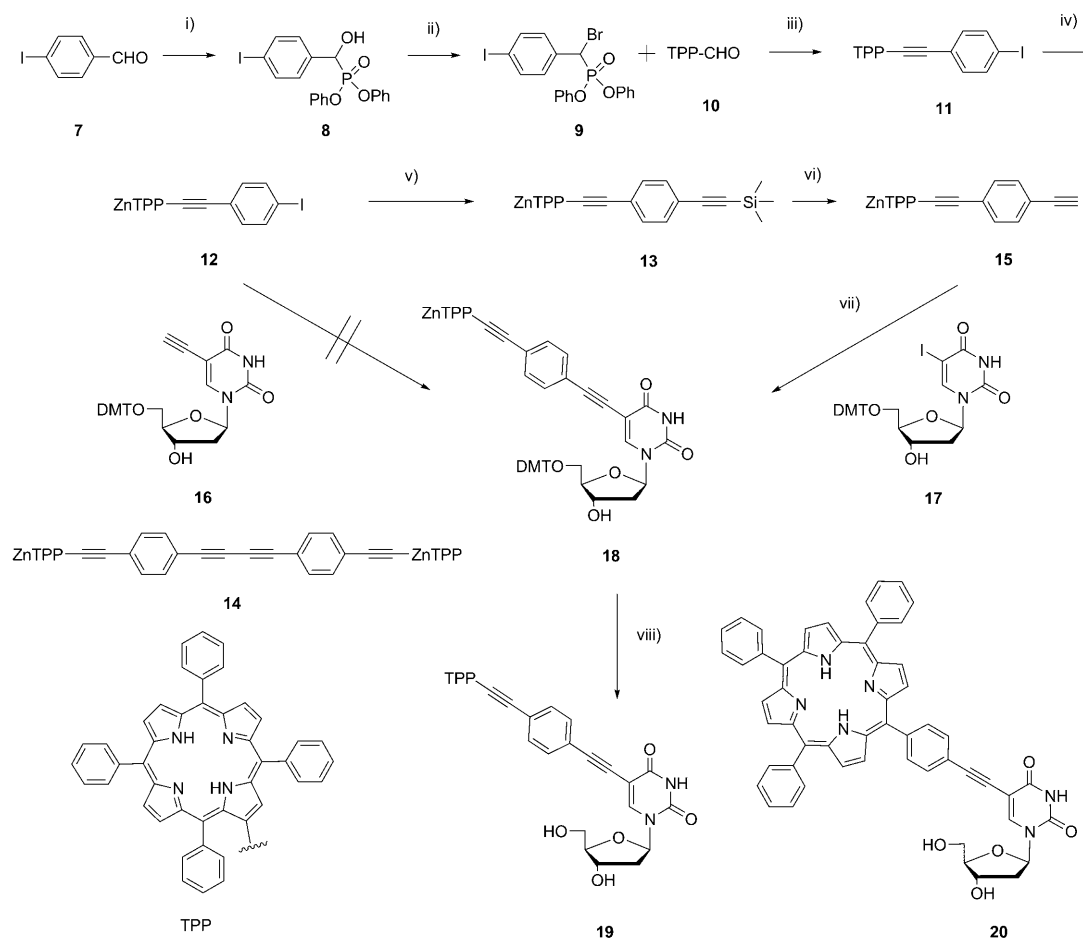
Apart from our recent publication,^[22] there has only been one other report of β -pyrrolic-substituted porphyrin in the structure of DNA.^[18] A flexible tether and phosphoramidite chemistry were used to place a porphyrin in the middle of a DNA duplex as a base substituent. We decided to investigate the possibilities of porphyrin covalent attachment to nucleosides through the β -pyrrolic position with the ultimate goal of creating DNA-based porphyrinic assemblies. To form a covalent linkage with nucleosides/DNA we considered two options that can be applied to either pre- or post-synthetic modification of DNA, that is, palladium(0)-catalysed Sonogashira and copper(I)-catalysed azide/alkyne cycloaddition.^[24] The synthesis of porphyrin precursors suitable for coupling reactions on nucleosides and DNA is described below and is based on the 2-formyl-5,10,15,20-tetra-

phenylporphyrin **10** (Scheme 2). This compound is easy to synthesise in high yields and multi-gram quantities without the need for difficult silica gel chromatography. This is in contrast to another building block used in β -pyrrolic functionalisation, 2-bromo-5,10,15,20-tetraphenylporphyrin. The radical bromination of 5,10,15,20-tetraphenylporphyrin (TPP) using *N*-bromosuccinimide (NBS) in organic solvents such as CHCl_3 ^[29] usually produces di- and tribrominated species along with the target compound, which is difficult to purify particularly during scaling up. The aldehyde in **10** serves as a useful functionality for the synthesis of different alkene and alkyne derivatives possessing a range of functional groups, which in turn can be used for covalent attachment to DNA. We assumed that variation of the porphyrin

attachment and positioning within the DNA structures is of interest due to the increased attention shown in recent years in macromolecular multi-chromophoric scaffolding in the field of material sciences.^[30]

Synthesis of porphyrin-2'-deoxyuridine conjugates using the

Sonogashira reaction: The β -functionalised porphyrin nucleoside **18** was synthesised in five steps from 2-formyl-5,10,15,20-tetraphenylporphyrin **10** (Scheme 2, see the Supporting Information for experimental procedures). Compound **10** was easily prepared according to the procedure of Bonfantini et al.^[31] in 85% overall yield in three steps by the quantitative insertion of copper(II) into TPP followed



Scheme 2. Reagents and conditions: i) diphenyl phosphite, MgO, RT, overnight, 90%; ii) CH₂Cl₂, DDQ, PPh₃, *n*Bu₄NBr, RT, overnight, 84%; iii) THF, *t*BuOK, RT, 3 h, 75%; iv) CHCl₃, MeOH, Zn(OAc)₂·2H₂O, RT, 1 h, 99%; v) Et₃N, trimethylsilylacetylene, [Pd(PPh₃)₄], CuI, reflux, 3 h, 93%; vi) CH₂Cl₂, THF, TBAF, RT, 5 min, 97%; vii) Et₃N, [Pd(PPh₃)₄], CuI, 70 °C, overnight, 78% crude, 12% pure; viii) CH₂Cl₂, TFA, RT, 2 min, 70%.

by Vilsmeier formylation and demetallation. Bromophosphonate **9**, required for the synthesis of **11**, was obtained from phosphonate **8** by using tetrabutylammonium bromide, DDQ and triphenylphosphine in 84% yield by using the method of Firouzabadi et al.^[32] Phosphonate **8** was synthesised in 90% yield by using diphenyl phosphite and 4-iodobenzaldehyde (**7**). The iodo-functionalised porphyrin **11** was obtained by a modified Horner–Emmons reaction^[33] of the bromophosphonate **9** and TPP-CHO (**10**) in 75% yield. This reaction could easily be scaled up to allow the multi-gram production of **11**. Zinc(II) was inserted into the porphyrin core to give **12** in quantitative yield to prevent copper insertion during the subsequent Sonogashira reactions in which copper(I) is used as a co-catalyst. Conversion of **12** into **13** was achieved in 93% yield by heating at reflux a solution of 2-(4'-iodophenyl)ethynyl-5,10,15,20-tetraphenylporphyrinatozinc(II) (**12**) and trimethylsilylacetylene in Et₃N in the presence of 0.3 equiv of [Pd(PPh₃)₄] and 0.5 equiv of CuI under argon overnight. The use of DMF as solvent resulted in the isolation of the starting material. It was critical to remove trace quantities of copper and palladium salts by washing the CH₂Cl₂ solution of trimethylsilyl-

protected porphyrin **13** repeatedly with 5% aq. Na₂EDTA solution followed by 3M NH₄OH. Failure to do so resulted in the exclusive formation of the Glaser homodimer byproduct **14** upon cleavage of the silyl protecting group. After washing, deprotection of **13** to **15** using TBAF was achieved with no sign of the unwanted Glaser homodimer **14**.

The target nucleoside **18** (Scheme 2) was synthesised from 2-(4'-ethynylphenyl)ethynyl-5,10,15,20-tetraphenylporphyrinatozinc(II) (**15**) and 2'-deoxy-5'-*O*-DMT-5-iodouridine (**17**) (DMT=4,4'-dimethoxytrityl) in high yield. Crucial to the success of the Sonogashira coupling reaction between **15** and **17** was the complete degassing of all the solvents and the use of at least 4 equiv of **17** to maximise the formation of **18**. It was also essential to mix both reactants in Et₃N before the addition of the palladium(0) and copper(I) catalysts. Failure to do so resulted in the formation of the homodimer **14**. Although the synthesis was successful, purification by silica gel chromatography was problematic and pure compound **18** was obtained in only 12% yield after subsequent methanol precipitation. Attempts to couple iodoporphyrin (**12**) and 2'-deoxy-5'-*O*-DMT-5-ethynyluridine (**16**) by using the same reaction conditions showed only trace

amounts of the desired product by TLC analysis of the reaction mixture. Demetallation and DMT deprotection of **18** performed in one step by using trifluoroacetic acid provided compound **19**, the spectroscopic properties of which were compared with the previously reported *meso*-linked uridine nucleoside **20**.^[5] In chloroform, the B band of the *meso*-uridine **20** was observed at 420 nm whereas that of the β -pyrrolic-functionalised **19** was detected at 429.5 nm. This 9.5 nm bathochromic shift in the B band of **19** is most likely a result of a higher degree of conjugation between the porphyrin core and uracil in comparison with **20**. To the best of our knowledge, this is the first reported synthesis of a β -pyrrolic porphyrin linked to a nucleobase. Owing to the unexpectedly low quantities of **18** obtained, conversion of pure **18** into the corresponding phosphoramidite was not attempted and efforts were focused on CuAAC and post-synthetic DNA modifications.

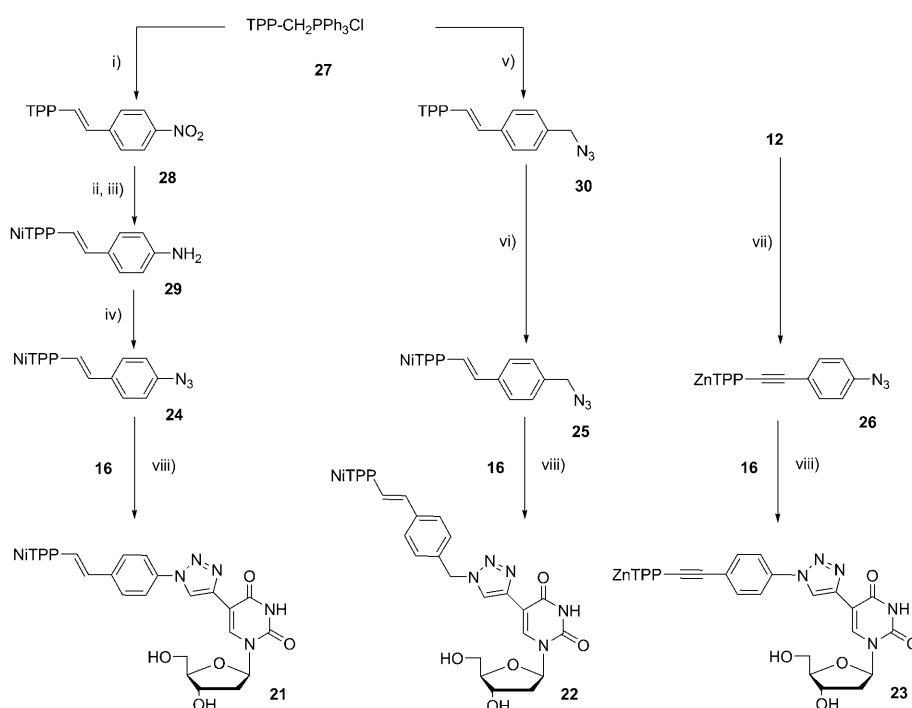
Synthesis of porphyrin-2'-deoxyuridine conjugates using CuAAC: Three different approaches were used to prepare the 1,4-regioisomeric 1,2,3-triazole-linked porphyrin nucleosides **21–23** (Scheme 3) as models for the post-synthetic CuAAC reactions. To demonstrate the versatility of the reaction three different porphyrin azides were chosen: the alkene-linked aromatic azide **24**, the more flexible alkene-linked aliphatic azide **25** and the acetylene-linked aromatic

azide **26**. Azides **24** and **25** were synthesised from the phosphonium salt **27**, which was obtained from TPP in six steps in an overall yield of 85% via the formation of TPP-CHO (**10**).^[34] Treatment of a CH₂Cl₂ solution of **27** with 4-nitrobenzaldehyde and 1,8-diazabicyclo[5.4.0]undec-7-ene (DBU) using a modification of the method of Bonfantini et al.^[31] resulted in the rapid formation of a *cis/trans* mixture of **28**, which was converted exclusively into the *trans* isomer by treatment with iodine in CHCl₃. Metallation of the nitro derivative **28** with Ni(OAc)₂·4H₂O provided the nickel(II) analogue, which was reduced to the amine **29** by using SnCl₂/HCl. Nickel(II) was inserted into the core of the porphyrin before the reduction of the nitro group to prevent insertion of tin during the reduction reactions and copper during subsequent CuAAC reactions. The β -functionalised aromatic azide **24** was prepared using a modified method^[35,36] by diazotisation with H₂SO₄/NaNO₂ in darkness followed by the addition of NaN₃.

The aliphatic azide **25**^[22] was synthesised by a Wittig reaction between phosphonium salt **27** and 4-(azidomethyl)benzaldehyde^[37] in the presence of DBU followed by isomerisation with iodine and nickel(II) insertion. The azide **26** was synthesised in 61% yield by the reaction of the iodo precursor **12** with NaN₃, sodium ascorbate, *N,N*-DMEA and Cu(ACN)₄PF₆ in dry DMSO. Alternative reaction conditions using CuI as catalyst or toluene as solvent resulted in the isolation of the starting material **12**.

The model triazoles **21–23**

were synthesised from the corresponding azides **24–26** and 2'-deoxy-5'-*O*-DMT-5-ethynyluridine (**16**) with 2 equiv of Cu(ACN)₄PF₆ in THF. This copper catalyst, which is soluble in organic solvents, was used as it had previously shown improved results in comparison with CuSO₄·5H₂O or CuI in CuAAC reactions.^[35] Silica gel TLC analysis of the reaction mixture showed the formation of a more polar material that moved either as one or two spots in MeOH/CH₂Cl₂ (1:19). This suggested the complete (**21**) or partial cleavage (**22** and **23**) of the DMT protecting group during the CuAAC reaction, which was confirmed by ¹H NMR spectroscopy and ESI-MS analysis of the intractable mixture. The desired triazoles were easily purified from the unreacted azides by silica gel column chromatography. As expected, reactions performed



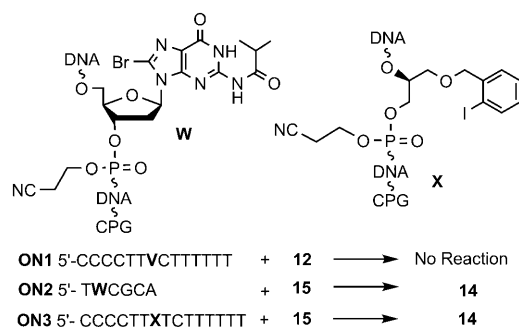
Scheme 3. Reagents and conditions: i) 4-nitrobenzaldehyde, DBU, CH₂Cl₂, RT, 30 min, then CHCl₃, I₂, RT, 3 h, 85%; ii) CHCl₃, MeOH, Ni(OAc)₂·4H₂O, reflux, overnight, quantitative; iii) THF, SnCl₂·2H₂O, HCl, RT, 48 h, 78%; iv) THF, H₂O, NaNO₂, H₂SO₄, RT, 2 h then NaN₃, RT, 20 min, 98%; v) 4-(azidomethyl)benzaldehyde, DBU, CH₂Cl₂, RT, 20 min, then CHCl₃, I₂, RT, overnight, 60%; vi) CHCl₃, MeOH, Ni(OAc)₂·4H₂O, reflux, overnight, 99%; vii) DMSO, NaN₃, sodium ascorbate, Cu(ACN)₄PF₆, *N,N*-DMEA, 70 °C, 48 h, 61%; viii) THF, Cu(ACN)₄PF₆, RT, 2–4 days, 36% for **21**, 28% for **22** and 39% for **23**.

with the free base azide **30** resulted in the quantitative isolation of the copper(II)-metallated porphyrinic azides with no triazole formation.

The spectroscopic properties of the porphyrin-linked uracil derivatives **21–23** were investigated and compared. In the UV/Vis spectra of compound **23** the porphyrin B band occurred at 435 nm. By comparison with the ethynyl derivative **18**, which has a B band at 440 nm, we can conclude that the introduction of the triazole in **23** leads to a loss of conjugation between uracil and the porphyrin. Similarly, a comparison of the aromatic triazole **21** with aliphatic triazole **22**, which show B bands at 427.5 and 426 nm, respectively, confirmed that the incorporation of CH₂ results in disruption of the remaining conjugation between the porphyrin core and the uracil.

Post-synthetic DNA modifications using the Sonogashira reaction: Post-synthetic oligonucleotide modification is an attractive alternative to the time-consuming preparation of multiple phosphoramidites. This is particularly important for screening various positions of the porphyrin moiety in the structure of DNA. In addition, due to the limited stability of porphyrin-containing phosphoramidites^[11,12] and difficulties in obtaining the pre-synthetic analogues in sufficient quantities, as discussed above, post-synthetic modification is clearly an option for porphyrin–DNA derivatives. Therefore we decided to investigate post-synthetic Sonogashira and CuAAC reactions as a means of creating porphyrin-modified ONs.

Previously, the palladium(0)-catalysed Sonogashira reaction was performed on a solid support of ONs possessing 5-iodopyrimidines,^[38] 8-bromopurines^[39] as well as 2- or 4-iodobenzyl- or 4-ethynylbenzylglycerols.^[28,40] No side-reactions were observed for native nucleobases with protecting groups.^[38] For the post-synthetic Sonogashira reaction using automated DNA synthesis we prepared 5'-DMT-on ONs **ON1–ON3** containing a single internal insertion of one of the following functionalised DNA building blocks: 2'-deoxy-5-ethynyluridine (**V**; Scheme 1), 2'-deoxy-8-bromoguanosine (**W**) or (*R*)-1-*O*-(2-iodobenzyl)glycerol (**X**; Scheme 4). The phosphoramidites required for oligonucleotide synthesis were either prepared, as in the case of 2'-deoxy-5-ethynyl-



Scheme 4. Reagents and conditions: compound **12** or **15**, [Pd(PPh₃)₄], CuI, DMF, Et₃N, 3 h.

uridine^[26] and (*R*)-1-*O*-(2-iodobenzyl)glycerol,^[28] or purchased, as in the case of 8-bromo-2'-deoxyguanosine.

We investigated the palladium(0)-catalysed Sonogashira reaction between CPG-bound oligonucleotides **ON2** and **ON3** and ethynyl-functionalised porphyrin **15** (Scheme 4). The reactions were carried out by using a protocol described earlier^[40] followed by cleavage of ONs from the CPG support using 32% NH₄OH. UV/Vis spectra of the ONs cleaved from the solid support showed traces of DNA–porphyrin conjugates, whereas TLC analysis of the reaction mixture after the Sonogashira reaction showed the exclusive formation of the Glaser homodimer **14** (Scheme 2). On the other hand, the iodo-porphyrin **12** was treated with **ON1** in a similar manner, because under these conditions the formation of the porphyrin homodimer is unfeasible. Unfortunately, no porphyrin-functionalised ONs were obtained. Because of the failures of the Sonogashira reaction we changed our approach and switched to the post-synthetic CuAAC reaction.

Post-synthetic DNA modifications using CuAAC: The copper(I)-catalysed Huisgen 1,3-dipolar cycloaddition,^[23] which is one of the variations of click chemistry, has been extensively used for the functionalisation of biomolecules,^[41] including the post-synthetic labelling of DNA.^[25] We prepared DMT-off ONs containing a single internal insertion of 2'-deoxy-5-ethynyluridine (**V**),^[26] (*R*)-1-*O*-(4-ethynylbenzyl)glycerol (**Z**)^[28,42] or commercially available 2'-*O*-propargyluridine (**Y**)^[27] (Table 1, **ON4–ON9**).

Table 1. ONs before and after CuAAC reactions with porphyrin azides **24** or **25**.^[a]

	Oligonucleotide (5'-3')	<i>m/z</i> [Da]		Retention time [min] ^[b]	Conversion [%] ^[c]
		calcd	found		
ON4	CCCCTTVCTTTTT	–	–	18.8	–
ON5	CCCCTTYCTTTTT	–	–	18.2	–
ON6	CCCCTTZCTTTTT	–	–	17.8	–
ON7	AGCTVGCTTGAG	–	–	20.8	–
ON8	AGCTYGCTTGAG	–	–	20.7	–
ON9	CTCAAGZCAAGCT	–	–	20.8	–
ON10	CCCCTT1CTTTTT	4958.9	4956.0	41.6	45
ON11	CCCCTT2CTTTTT	4972.9	4961.7	41.7	48
ON12	CCCCTT3CTTTTT	4988.9	4979.8	42.0	64
ON13	CCCCTT4CTTTTT	5002.9	4997.4	40.8	71
ON14	CCCCTT5CTTTTT	5216.9	5202.8	43.2	60
ON15	CCCCTT6CTTTTT	5231.0	5229.9	42.6	58
ON16	AGCT1GCTTGAG	4497.8	4507.0	45.1	31
ON17	AGCT2GCTTGAG	4511.9	4517.2	45.0	55
ON18	AGCT3GCTTGAG	4527.8	4525.9	46.2	60
ON19	AGCT4GCTTGAG	4541.8	4541.4	45.2	67
ON20	CTCAAG5CAAGCT	4693.9	4697.2	47.0	19
ON21	CTCAAG6CAAGCT	4707.9	4707.9	46.7	39

[a] Post-synthetic CuAAC reactions: DNA on CPG (0.33 μmol), azide **24** or **25** (7.67 μmol), CuSO₄·5H₂O (0.2 μmol in 5 μL H₂O), sodium ascorbate (1.0 μmol in 20 μL H₂O), DMSO (150 μL), shaking, RT, 3 days. [b] Retention times ±0.5 min, see the Experimental Section for HPLC gradients. [c] The conversions of DNA were determined from the HPLC peak integrals at 260 nm.

CuAAC reactions were carried out by mixing nickel-containing porphyrin azide **24** or **25** (7.67 μmol) and one of the alkyne CPG-bound oligonucleotides **ON4–ON9** (0.33 μmol) in a micro-centrifuge vial followed by the addition of DMSO (150 μL) to dissolve the azide. Freshly prepared $\text{CuSO}_4 \cdot 5\text{H}_2\text{O}$ (0.2 μmol in 5 μL H_2O) and sodium ascorbate (1.0 μmol in 20 μL H_2O) solutions were added, which resulted in the partial precipitation of the porphyrin azide. The reaction vessels were then sealed under argon to avoid DNA cleavage caused by copper ions in the presence of oxygen^[43] and shaken at RT for 3 days. After shaking, the CPG supports were repeatedly washed with CH_2Cl_2 to remove unreacted azide. The resulting red-coloured CPG support provided an indication of the progression of the reaction. The unreacted azide was recovered in 80–90% yield for use in future coupling reactions by washing the CH_2Cl_2 solution containing the azide with H_2O followed by drying over MgSO_4 and precipitation from $\text{CH}_2\text{Cl}_2/\text{MeOH}$. ONs were then cleaved from the solid support (32% NH_4OH) and purified by semi-preparative HPLC on a C_{18} column. Porphyrin-conjugated ONs showed appreciably higher retention times than unmodified oligonucleotides (Table 1 and Figure 1 in the Supporting Information) and ONs possessing 2'-*O*-propargyluridine (**Y**) showed superior conversions in comparison with ONs containing 2'-deoxy-5-ethynyluridine (**V**) and (*R*)-1-*O*-(4-ethynylbenzyl)glycerol (**Z**). Mixed purine/pyrimidine sequences **ON16–21** were found to have lower conversions than pyrimidine sequences **ON10–15**. For the incorporation of multiple porphyrins into DNA a protocol was developed^[22] in which focused microwave irradiation^[44,45] (20 min at 70 °C) resulted in the complete conversion of alkyne-DNA.

After HPLC purification, the collected fractions were lyophilised, redissolved in 100 μL of H_2O and precipitated from $\text{LiClO}_4/\text{acetone}$ to give a deep-red pellet. The pellet was dissolved in 100 μL of H_2O to create stock solutions (ca. 300–1000 μM). Not all ON precipitates completely dissolved in water (100 μL) and heating at 70 °C for several hours was required to increase solubility. ONs were desalted using C_{18} zip-tips and then characterised by MALDI-TOF MS (Table 1). The purity was checked by using 20% denaturing polyacrylamide gel electrophoresis (PAGE; 7M urea), which showed a single red band with significant retardation compared with the wild-type ON (Figure 1). This is in contrast to the work published by Fendt et al., which showed increased mobility of ONs possessing a single porphyrin moiety compared with the wild-type ON.^[5]

Single-stranded porphyrin-ONs: Single-stranded **ON10–ON21** were prepared as 1.0 μM solutions in cacodylate buffer at various pH (5.0, 6.0 and 7.2). The CD spectra of all the porphyrin-modified ONs at pH 6.0 showed signals in the region typical of DNA nucleobases at 248 (–ve ellipticity) and 280 nm (+ve ellipticity, not shown).^[46] Strong signals arising from the absorbance of the porphyrin Soret band were observed including the formation of bisignate curves, which is an indication of the existence of exciton coupling

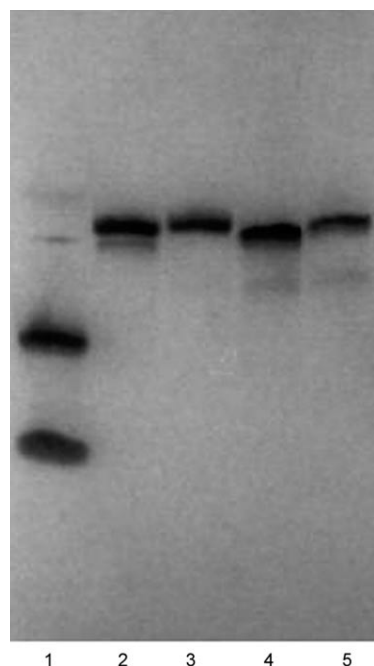


Figure 1. Denaturing 20% PAGE (7M urea) of porphyrin-ONs stained with Stains-All and destained in H_2O . Porphyrin-modified ONs were red before staining. Lane 1 is unmodified oligonucleotide **ONwt** (top) and a colour marker (Bromophenol Blue, bottom), lane 2 is **ON17**, lane 3 is **ON16**, lane 4 is **ON19** and lane 5 is **ON21**.

between porphyrins (see Figure 2 of the Supporting Information).

Further analysis revealed that the CD signals are pH-dependent for the CT sequences (**ON10–15**) but not for the mix-mers **ON16–21**. For example, the CT sequence **ON15** showed virtually no CD signals in the porphyrin region at pH 7.2, whereas a strong bisignate curve was observed at pH 5.0 and 6.0 (Figure 2A). In addition, the CD intensity in the UV region decreased with increasing pH and was blue-shifted by 6 nm. This is a characteristic CD signature of i-motifs,^[47] which are formed by the base-pairing of hemi-protonated cytosine⁺ and cytosine to form duplex structures that are zipped together in an anti-parallel orientation.^[48] This topology is enabled by the N3-protonation of cytosine, which forms three hydrogen bonds with another cytosine. Depending on the ionic strength, the pK_a of cytosine in i-motifs varies between 4.5 and 4.8,^[49] which makes these structures unstable at higher pH. It is important to note that the CD signals of unmodified CT-**ONwt** (Table 2, see later) did not show the characteristic pH dependency (Figure 2B), which suggests that the porphyrin triggers the formation of i-motifs for the sequence containing a run of only four cytosines. An increase in the pH from 5.0 to 7.2 led to cytosine deprotonation, i-motif unfolding and loss of porphyrin–porphyrin interactions. We assume that i-motif formation allowed the orientation of porphyrins in such a manner that porphyrin–porphyrin exciton coupling occurred through porphyrin stacking, as shown in the plausible i-tetraplex structure (Figure 2D). Native PAGE (pH 5.0) confirmed the ab-

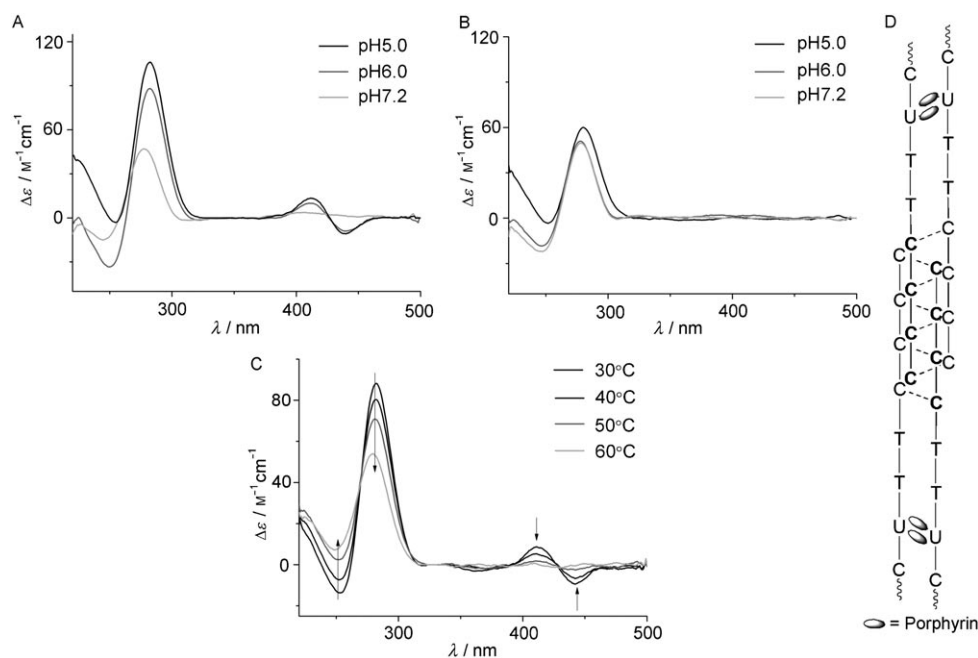


Figure 2. A) CD spectra of single-stranded oligopyrimidine **ON15** at pH 5.0, 6.0 and 7.2. B) CD spectra of **ONwt** at pH 5.0, 6.0 and 7.2. C) CD thermal melting of single-stranded oligopyrimidine **ON15** at pH 5.0. D) Possible i-tetraplex formation. Buffers contain 20 mM sodium cacodylate, 100 mM NaCl and 5 mM MgCl₂.

sence of an i-motif for **ONwt**, whereas CT-ONs with porphyrins did not penetrate into the 20% native gel at pH 5.0 (gel not shown). This was also true with a decreased percentage of acrylamide gels (8 and 12%). We recently observed^[22] that short DNAs (12–20-mers) with more than two porphyrins in their structures do not penetrate into native and denaturing PAGEs, possibly as a result of aggregation in the gel well. In the present case a significant retardation of porphyrin DNAs compared with that observed in denaturing PAGE confirms the formation of a secondary structure (i-motif).

Thermal melting of the single-stranded ONs resulted in the loss of the CD signal at around 430 nm and reduced signal intensity at 280 nm (Figure 2C), which suggests the melting of i-motifs (**ON10–ON15**) and the separation of aggregates. We performed CD thermal denaturation of single-stranded **ON10**, **ON12** and **ON14** at pH 5.0 and found that irreversible melting occurred with mid-transition temperatures ($T_{1/2}$) of 51, 52 and 56 °C, respectively (Table 1 of the Supporting Information). After melting, the porphyrinic CD signal was observed only after incubation at 20 °C overnight and with an intensity significantly lower than that of unheated samples. This means that the formation of porphyrinic i-motif aggregates is slow at 1.0 μM and that aggregates presumably form in the concentrated stock solution (ca. 300–1000 μM). To the best of our knowledge this is the first observation of ON aggregation/i-motif formation as a result of internal incorporation of a single porphyrin in the sequence. The pH-independent CD spectra observed for mix-mers (see Figure 3 of the Supporting Information) suggest the formation of aggregates rather than i-motifs in sequences

ON16–21. Recently, intermolecular, end-to-end porphyrin–porphyrin stacking between DNA duplexes and, consequently, distinctive multi-signate CD signals in the porphyrin Soret band region were observed for duplexes possessing a porphyrin at the 5'-end at high ionic strength (150 mM NaCl for copper–porphyrin, 450 mM for zinc–porphyrin).^[19,21] Clearly, porphyrin–porphyrin intermolecular interactions in the DNA structures are strongly dependent upon the ON sequence, the length, the porphyrin insertion and the ionic strength. For instance, in the course of our study of purine–pyrimidine 18-mer DNA possessing modification **4** in the middle of the sequence,^[22] we did not observe aggregate formation for single-stranded ONs probably due to increased electrostatic repulsion between negatively charged phosphates. For comparison, our CT sequence is 14-mer and our mix-mer sequence studied here is 12-mer. Nevertheless, the aggregation of the ONs described herein was found to be slow after heating our samples at 90 °C for 5 min and thus it should not affect the formation of duplexes and triplexes.

DNA duplexes and triplexes: The thermal stability of duplexes and triplexes containing the synthesised oligonucleotides **ON10–ON21** was assessed by UV/Vis thermal denaturation experiments in the range 10–70 °C at 260 and 430 nm. The melting temperatures (T_m) were determined as the maxima of the first derivatives of the melting curves and they are listed in Tables 2 and 3 (annealing temperatures are listed in Tables 2 and 3 of the Supporting Information). Sequences possessing different porphyrin modifications were studied in a parallel duplex with the duplex **D1** and in anti-parallel duplex with appropriate oligonucleotides **ON22–24**.

Table 2. Melting temperatures of porphyrin-containing parallel triplex and anti-parallel duplex.^[a]

Sequence (5'-3')	Parallel triplex ^[b] 3'- CTGCCCTTTCTTTT/5'-GACGGG- GAAAGAAAAA (D1)		Anti-parallel duplex ^[c] 3'- GGGAAAGAAAAA (ON22)	
	pH 5.0	pH 6.0	pH 6.0	pH 7.2
ONwt CCCCTTTCTTTT	54.0 ^[d]	27.0	48.0	48.0
ON10 CCCCTT1CTTTT	39.0 (39.0)	39.0 (37.0)	31.0 (30.0)	30.0 (30.3)
ON11 CCCCTT2CTTTT	40.0 (39.5)	30.0 (37.7)	32.5 (29.0)	33.2 (33.7)
ON12 CCCCTT3CTTTT	54.5 ^[d] (53.5)	34.5 (29.3)	35.0 (28.5)	33.2 (33.7)
ON13 CCCCTT4CTTTT	55.0 ^[d] (54.0)	34.5 (32.7)	41.5 (43.8)	41.7 (43.0)
ON14 CCCCTT5CTTTT	55.0 ^[d] (53.0)	38.9 (37.0)	38.7 (24.0)	34.6 (37.0)
ON15 CCCCTT6CTTTT	55.0 ^[d] (53.5)	36.3 (36.8)	33.3 (31.0)	34.3 (34.6)

[a] T_m [°C] data for parallel triplex and anti-parallel duplex melting, taken from the UV/Vis melting curves at 260 and 430 nm (shown in parentheses). [b] 1.5 μM of **ON10–15** and **ONwt** and 1.0 μM of each strand of dsDNA (**D1**) in 20 mM sodium cacodylate, 100 mM NaCl and 5 mM MgCl_2 , pH 5.0 and 6.0. [c] 1.0 μM of each strand in 20 mM sodium cacodylate, 100 mM NaCl and 5 mM MgCl_2 , pH 6.0 and 7.2. [d] Third strand and duplex melting overlaid.

As can be seen from the T_m data in Table 2, the internal insertion of a porphyrin resulted in increased T_m values ($\Delta T_m = 3.0\text{--}12.0^\circ\text{C}$) of the Hoogsteen-type triplexes relative to the wild-type triplex **ONwt/D1** at pH 6.0. The TFO strands **ON10** and **ON14** containing aromatic porphyrins (modifications **1** and **5**, Scheme 1) resulted in slightly greater stabilisation of the triplex at pH 6.0 compared with **ON11** and **ON15** containing the aliphatic-linked porphyrins (modifications **2** and **6**). Note that the pH dependence of triplex thermal stability is less pronounced for triplexes in which the porphyrin is linked to the 5-position of uridine (**ON10/D1** and **ON11/D1** versus **ON12–ON15/D1**, pH 5.0 and 6.0). This can be explained by molecular modelling (AMBER* force field,^[50] Figure 3). The porphyrins in modifications **1** and **2** are located in the major groove of the duplex, occupying the space between the TFO and the homopyrimidine strand of the duplex **D1** (Figure 3A). This means that the porphyrin, especially in the case of aliphatic modification **2**, is located close to the nucleobases. This hydrophobic effect alters the hydration of the triplex and might have an influence on the pK_a values of cytidines nearby, thus changing the response of the triplex to pH. In contrast, the porphyrins in modifications **3** and **4** are located away from the nucleobases on the edge of the homopurine strand of the duplex and the TFO with very little influence on the hydration of the major groove of the DNA (Figure 3B). Aliphatic porphyrins provide greater flexibility in comparison with aromatic porphyrins, which results in closer interactions between the porphyrin and the triplex (see Figure 5 of the Supporting Information). We performed thermal stability studies on triplexes having a single mis-match with **ON10–13** and found that no triplexes are formed at pH 5.0 (data not shown). This means that there is no intercalation of the porphyrin in triplexes **ON10–13/D1**, in accord with results of the molecular modelling. In the case of **ON14** and **ON15**, in which the porphyrin is incorporated as a bulged insertion into the triplex strands, the porphyrin may either penetrate through the DNA duplex (Figure 3C) or intercalate between bases in the duplex such that the *meso*-phenyl rings are located in the grooves of the triplex (Figure 3D). These

two orientations are possible as a result of the long linker between the porphyrin and the phosphate backbone (19 Å). Intercalation, similar to that shown in twisted intercalating nucleic acids (TINA) configurations,^[44] was found to be of higher energy ($-20034\text{ kJ mol}^{-1}$, Figure 3B) than when the porphyrin penetrates the duplex strands and aligns itself in the minor groove ($-20086\text{ kJ mol}^{-1}$, Figure 3C).

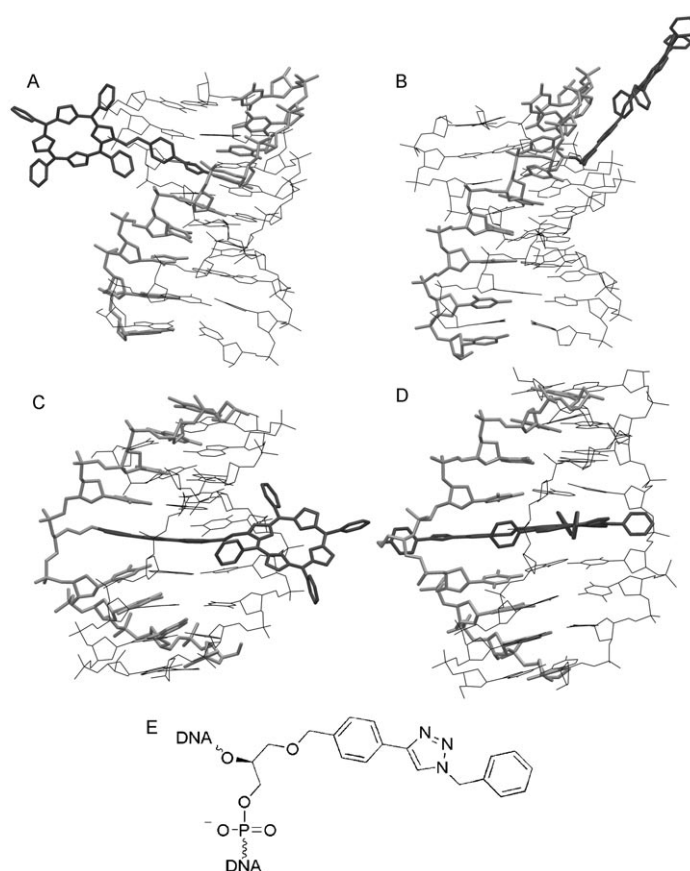


Figure 3. Representations of the lowest-energy structures of triplexes **ON10/D1** (A), **ON12/D1** (B) and **ON14/D1** (C, D) possessing aromatic porphyrins **1**, **3** and **5**, respectively. Two possible porphyrin orientations are shown for the triplex **ON14/D1**: C) The porphyrin penetrating through the duplex **D1**. D) The higher-energy structure in which the porphyrin intercalates between the bases of duplex **D1**. E) 1,2,3-Triazole-linked benzyl moiety incorporated into TFO as a bulge.^[44]

This difference in energy is most likely a result of the destabilising bulge in the phosphate backbone of the TFO strand, which is required for porphyrin intercalation between the bases of the duplex strands. Further thermal stabi-

lisation might be possible by reducing the length of the linker, which reduces the bulge in the backbone of the TFO strand.

As expected, the T_m values of the triplexes of **ON12–15/D1** increased at pH 5.0 due to increased cytosine protonation. Surprisingly, the T_m values of **ON10** and **ON11** were almost unchanged. No triplex formation was observed above 10 °C at pH 7.2. The importance of the porphyrin in the stability of the triplex can be emphasised when we compare the previously reported T_m value for the bulged insertion of the 1,2,3-triazole-linked benzyl moiety (Figure 3E) in the TFO strand.^[44] Under identical conditions and by using the sequence equivalent to **ON15**, destabilisation of the resulting triplex by more than 23 °C was observed at pH 6.0.

To confirm triplex formation, the CD spectra of the triplexes were recorded at pH 5.0 and 6.0. A strong negative band at 209 nm was observed (see Figure 4 of the Supporting Information), which confirms the formation of a triplex^[51] in porphyrin-modified sequences.

It was observed (Table 2) that a single internal incorporation of a porphyrin in an anti-parallel duplex (**ON10–15/ON22**) resulted in the thermal destabilisation of the duplex compared with the unmodified duplex. Variation of the destabilisation depended on the porphyrin incorporated and its location in the duplex. We found that duplexes involving **ON10,11,14,15** showed a significant drop in thermal stability of 13.4–18.0 °C per modification at pH 7.2. Molecular modelling of these duplexes (Figure 4) suggest that the porphyrins have very little interaction with the nucleobases and are positioned in the major groove. As a result of the linker length, porphyrins **5** and **6** protrude through the duplex into the major groove, leaving just the phenyl and triazole moieties located between the bases in the duplex core. This intercalation may account for the slight duplex stabilisation of

ON14,15/ON22 over **ON10,11/ON22**. As the porphyrin is a hydrophobic moiety it could be expected that the destabilisation observed is a result of a significantly changed hydration of the duplex in comparison with the wild-type duplex.

Significant differences were found in the melting temperatures of duplexes containing **ON12** and **ON13** in which the porphyrin is positioned in the minor groove. Duplexes containing the aromatic porphyrin **3** (**ON12**) show ΔT_m values of –13.0 to –14.8 °C, respectively at pH 6.0 and 7.2, similar to the duplexes **ON10,11,14,15/ON22**, whereas duplex **ON13/ON22**, which contains the aliphatic porphyrin **4**, has a ΔT_m of –6.3 to –6.5 °C. Molecular modelling shows that the aromatic (**ON12**, Figure 4B) and aliphatic porphyrins (**ON13**, Figure 4E) follow the minor groove in a similar manner. However, the aliphatic porphyrin is less destabilising, presumably due to rotational flexibility around the extra sp^3 carbon which results in a better fit within the minor groove in comparison with the aromatic porphyrin.

Duplexes containing mixed purine/pyrimidine strands (Table 3) show a destabilisation trend similar to the porphyrin-modified CT sequences. Thus, significant thermal destabi-

Table 3. Melting temperatures of anti-parallel duplexes containing mixed purine/pyrimidine strands.^[a]

	Sequence (5'-3')	Anti-parallel duplex 3'-TCGAAC- GAACTC (ON23)		Anti-parallel duplex 3'-GAGTTCGTT- GA (ON24)	
		pH 6.0	pH 7.2	pH 6.0	pH 7.2
ONwt_m	AGCTTGCTTGAG	50.0	50.0	–	–
ON16	AGCT1GCTTGAG	35.0 (32.0)	35.0 (34.0)	–	–
ON17	AGCT2GCTTGAG	34.0 (33.5)	32.0 (NVT) ^[b]	–	–
ON18	AGCT3GCTTGAG	36.0 (36.0)	34.0 (35.0)	–	–
ON19	AGCT4GCTTGAG	42.0 (39.0)	43.0 (NVT) ^[b]	–	–
ON20	CTCAAG5CAAGCT	–	–	32.0 (33.0)	33.3 (NVT) ^[b]
ON21	CTCAAG6CAAGCT	–	–	29.0 (28.0)	27.9 (29.1)

[a] T_m [°C] data for anti-parallel duplex melting, taken from the UV/Vis melting curves at 260 and 430 nm (shown in parentheses). 1.0 μM of each strand in 20 mM sodium cacodylate, 100 mM NaCl and 5 mM MgCl₂, pH 6.0 and 7.2.
[b] NVT = no visible transition.

bilisation was found for duplexes containing bulge insertions of porphyrin-glycerol moieties (**ON20** and **ON21** with **ON24**). Minor groove modification with the aliphatic porphyrin **4** resulted in the least destabilised duplex (**ON19/ON23**). In addition, the melting profiles (see Tables 2 and 3 of the Supporting Information) show virtually no hysteresis at either 260 or 430 nm for all duplexes, which indicates that the kinetics of both the denaturing and annealing processes are fast in comparison with the temperature gradient.

The CD spectra of duplexes containing **ON10–21** show a negative band at around 245–250 nm and a positive band at 274–280 nm (see Figure 6 of the Supporting Information), which clearly suggests that the modified duplexes retain

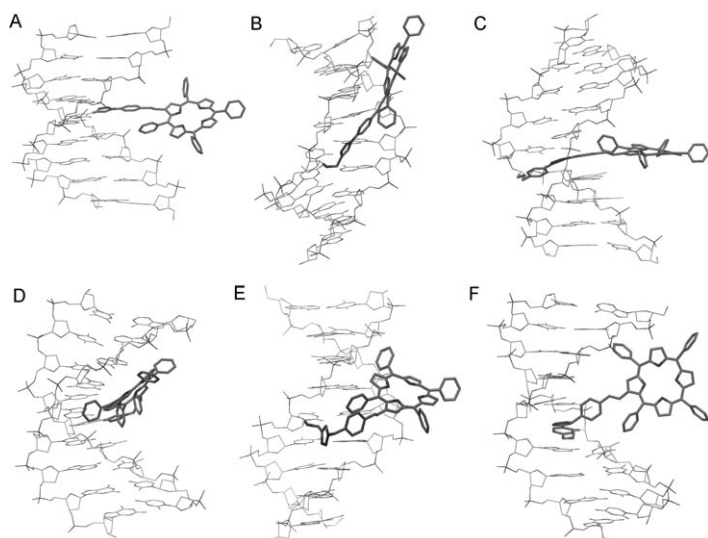


Figure 4. Representations of the lowest-energy structures of the duplexes formed by **ON10** (A), **ON12** (B), **ON14** (C), **ON11** (D), **ON13** (E) and **ON15** (F) with **ON22**.

their overall B-form double-helix structure. A CD signal in the porphyrin Soret band region was also observed for these duplexes either as a weak band or as a bisignate curve. In contrast to the CD spectra of single-stranded CT sequences, signals of duplexes in the porphyrin region returned to the pre-melted level almost instantaneously after samples were heated and cooled. Moreover, marginal changes in the CD profiles were observed by using lower or higher NaCl concentrations (50 or 500 mM, respectively, data not shown). Thus, duplex aggregation triggered by porphyrins, which should occur over longer periods of time and at high salt concentrations, was thought unlikely to happen. The presence of these CD signals, especially for constructs possessing a methylene group between a porphyrin and a nucleotide, led to the conclusion that the porphyrin interacts with the chiral environment of DNA.

Conclusion

We have investigated two routes of attachment of β -pyrrolic-substituted porphyrins to nucleosides and DNA. Several 2'-deoxyuridine derivatives were synthesised by either Sonogashira or CuAAC reactions. A higher degree of conjugation between uracil and the porphyrin core connected through a 1,4-diethynylbenzene moiety (**19**) was observed in the UV/Vis spectrum in comparison with the previously studied *meso*-functionalised porphyrin (**20**) linked at the 5-position of 2'-deoxyuridine. However, due to a low yields of porphyrin-nucleosides by the Sonogashira reaction we switched our focus to CuAAC coupling, which led to nucleoside and DNA conjugates modified with azidostyryl and methylazidostyryl-substituted nickel(II) porphyrins. We screened the effect of various single porphyrin modifications on the structures and thermal stability of single-stranded ONs and duplex and triplex DNAs. Three types of DNA building blocks with terminal alkynes were considered for CuAAC coupling to DNA: 2'-deoxy-5-ethynyluridine, 2'-*O*-propargyluridine and (*R*)-4-ethynylphenylmethylglycerol. Single-stranded ONs containing internal porphyrin modifications formed porphyrin-driven *i*-motif structures in pyrimidine sequences having a single terminal run of four cytosines. Porphyrin–porphyrin intermolecular interactions were also detected for purine/pyrimidine sequences. In both cases, the formation of aggregates/*i*-motifs was slow at room temperature after heating samples at 95 °C for 5 min. Thermal stability studies were performed on Hoogsteen-type triplexes containing porphyrin-modified TFO strands and it was found that porphyrin modifications generally stabilise the triplex in the ΔT_m range of +3 to +12 °C. This shows that 2'-deoxy-5-ethynyluridine and 2'-*O*-propargyluridine are promising as 'clickable' nucleotides for labelling with organic chromophores in internal positions of TFOs. Duplex thermal stability studies revealed that the aliphatic porphyrin **25** internally connected to the 2'-position of uridine destabilises duplexes to a lesser extent than other modifications. According to molecular modelling studies, porphyrins were

positioned in the minor groove of the duplex when attached to the 2'-*O*-position of the uridine. In contrast, porphyrin attachment at the 5-position of uridine or its use as an intercalating moiety led to duplexes with porphyrin in the major groove with no or very few interactions with nucleobases. Presumably, the additional flexibility provided by two methylene linkages in compound **4** helps the porphyrin to fit better within the minor groove of the duplex in comparison with the aromatic porphyrin **3**. These findings highlight the difference between the positioning of porphyrins in different DNA environments and thus they can be used in the construction of DNA-based photonic devices.

Experimental Section

Solid-phase synthesis of oligonucleotides and post-synthetic CuAAC: DMT-off oligodeoxynucleotides were synthesised by using MerMade 4 Automated DNA Synthesiser from BioAutomation Corporation on a 1.0 μ mol scale on 1000 Å CPG supports using 4,5-dicyanoimidazole as an activator and 0.075 M solutions of the corresponding phosphoramidites of **V**, **Y** and **Z** in dry MeCN with an increased coupling time (2 min). After DNA synthesis, DMT-off **ON4–ON9** on CPG (0.33 μ mol) containing **V**, **Y** or **Z** were removed from their corresponding columns and added to a microcentrifuge vial (1.5 mL) followed by the appropriate azide (7.67 μ mol, 23 equiv) in degassed DMSO (150 μ L). Freshly prepared $\text{CuSO}_4 \cdot 5\text{H}_2\text{O}$ (0.2 μ mol, 0.6 equiv, 5 μ L of a 40 mM solution in degassed H_2O) and sodium ascorbate (1.0 μ mol, 3 equiv, 20 μ L of a 50 mM solution in degassed H_2O) were added. The reaction mixture was shaken over argon in darkness for 3 days. CH_2Cl_2 (1 mL) was added to the reaction mixture and the CPGs were centrifuged (14500 rpm for 1 min). The solvents were removed and washing was repeated until the supernatant no longer showed any colour (see recovery of porphyrin azides). The red CPG was then washed with H_2O (1.5 mL) to remove any remaining inorganic salts. Residual solvent was removed under reduced pressure and the obtained DMT-off oligonucleotides bound to CPG supports were treated with 32% aq. NH_4OH (1 mL) at RT for 2 h and then at 55 °C overnight. The porphyrin-functionalised DMT-off ONs were purified by using a Waters 600 HPLC apparatus fitted with a Waters 2487 dual λ absorbance detector (260 and 427 nm) with a reversed-phase semi-preparative Econosil C_{18} (10 μ m, 10 \times 250 mm) column. Buffer A (0.05 M triethylammonium acetate in H_2O , pH 7.0) and buffer B (75% CH_3CN in H_2O), flow 2.5 mL min⁻¹. Gradients: 2 min 100% A, linear gradient to 70% B in 38 min, linear gradient to 100% B in 7 min, 100% B in 3 min and then 100% A in 10 min. After purification, the corresponding fractions were lyophilised, dissolved in H_2O (100 μ L), heating to 70 °C for 1 h was required to dissolve some ONs), 0.01 M lithium perchlorate in acetone (1.6 mL) was added and the ONs were stored at –10 °C for 1 h. The precipitated ON pellet was centrifuged (15000 rpm for 30 min), the supernatant removed and the pellet was washed with acetone (30 μ L). The molecular weights of the oligonucleotides were obtained by using a Bruker Daltonics Autoflex MALDI-TOF spectrometer in the negative mode using either 2',4',6'-trihydroxyacetophenone, 3-hydroxypicolinic acid or 6-azathiothymine matrices and dibasic ammonium citrate or 1*H*-imidazole as co-matrix. Oligonucleotides were desalted by using C_{18} ZipTips (Millipore) prior to loading on the MALDI plate. The purity was checked by using denaturing 20% PAGE (7 M urea), which showed a single red band with significant retardation relative to the wild-type oligonucleotide.

Recovery of azides: H_2O (50 mL) was added to the combined CH_2Cl_2 washings containing the reacted porphyrin azide and the resulting solution was vigorously stirred for 1 h. The organic layer was extracted into CH_2Cl_2 (2 \times 50 mL), dried over MgSO_4 , filtered and the porphyrin was precipitated from $\text{CH}_2\text{Cl}_2/\text{MeOH}$. The desired product was collected by filtration to give a red solid (approximately 80–90% recovery).

UV/Vis spectroscopic melting temperature measurements: Melting temperatures for duplexes and triplexes were measured with a CARY 100Bio UV/Vis spectrophotometer using a 2 \times 6 Multicell block with Peltier temperature controller. The triplexes were formed by first mixing the two strands of the Watson–Crick duplex, each at a concentration of 1.0 μ M, in the corresponding buffer solution followed by the addition of the third TFO strand at a concentration of 1.5 μ M (total volume 1 mL). The solutions were then heated at 90 $^{\circ}$ C for 15 min, cooled and incubated at 10 $^{\circ}$ C for 30 min. The duplexes were formed by mixing the two strands, each at a concentration of 1.0 μ M, in the appropriate buffer (total volume 1 mL). The solutions were heated at 90 $^{\circ}$ C for 15 min, cooled and incubated at 10 $^{\circ}$ C for 30 min. The melting temperatures were determined as the maxima of the first derivative plots of the melting curves obtained by measuring the absorbance at 260 and 430 nm against increasing temperature (10–70 $^{\circ}$ C, 1.0 $^{\circ}$ Cmin $^{-1}$ for duplexes and 10–70 $^{\circ}$ C, 0.5 $^{\circ}$ Cmin $^{-1}$ for triplexes). All melting temperatures were an average of two denaturing/annealing cycles. Extinction coefficients for porphyrin-modified oligonucleotides were calculated by using the extinction coefficients of each nucleoside at 260 nm. Extinction coefficients for porphyrin modified-nucleosides at 260 nm: **1**, 14800; **2**, 14800; **3**, 15900; **4**, 15900; **5**, 9000; **6**, 9000 L mol $^{-1}$ cm $^{-1}$.

Circular dichroism measurements: CD spectra were recorded using an Applied Photophysics Chirascan CD spectrometer (150 W Xe arc) with a Quantum Northwest TC125 temperature controller. Solutions containing 1.0 μ M of each strand were used for CD spectroscopy. An average of 10 scans was recorded (1 nm intervals, 240 nm min $^{-1}$, 1 cm pathlength), baselined against the appropriate buffer solution and then smoothed. Data were recorded in mdeg and converted into $\Delta\epsilon$. CD spectroscopic melting temperature measurements of i-motifs were performed by using solutions containing the appropriate strand at a concentration of 1.0 μ M in pH 5.0 buffer. Melting temperatures were determined from the maxima of the first derivative curves measured at 283 nm against increasing temperature (25–90 $^{\circ}$ C at 5 $^{\circ}$ C intervals with 300 s equilibration time).

Molecular modelling: Molecular modelling calculations and duplex construction were performed by using MacroModel v9.8 from Schrödinger. All calculations were performed by using the AMBER* force field^[50] and the GB/SA water model.^[52] The 8-mer duplexes containing unmetallated tetraphenylporphyrin-modified nucleotides were generated from a B-type DNA–DNA duplex by using Maestro v9.8 from Schrödinger. Parallel triplexes were constructed by consecutive superimposition of CGC and TAT triplets, which were generated with Insight II v9.72 from MSI^[51] and transported into MacroModel. Bulged insertions **5** and **6** were constructed in several steps. The unmodified duplex or triplex was constructed and the appropriate strand was disconnected by removal of the phosphate group at the location of the bulged insertion. Afterwards, the bulged insertion up to and including the triazole ring was constructed and placed between bases in the structure. The phosphate backbone was reconnected and minimisation was then performed, creating enough space for the bulged insertion. The appropriate porphyrin was then linked the triazole ring. Constraints ensured the planarity of the porphyrins and were based on the metal-complexed porphyrin available in the Maestro software (distances: N1–N3, N2–N4 4.132 Å ; force constant 100 kJ mol $^{-1}$ Å^{-2} ; torsion angles: N1–C2–C3–C4, N2–C6–C7–C8, N3–C10–C11–C12, N4–C14–C15–C16 0.0 $^{\circ}$; force constant 100 kJ mol $^{-1}$ Å^{-2}). Stochastic dynamics calculations generating 250 structures were performed by using an extended cut-off potential with a SHAKE algorithm to constrain bonds to hydrogen atoms. The simulation temperature was 300 K, the simulation time 500 ps and the equilibration time 150 ps. All 250 structures were minimised by using the Polak–Ribiere Conjugate Gradient (PRCG) method with a convergence threshold of 0.05 kJ mol $^{-1}$ and examined with XCluster from Schrödinger to find representative low-energy structures.

Acknowledgements

This work was financially supported by Marsden grants administrated by the Royal Society of New Zealand (grants nos. MAU0407 and MAU0704).

- [1] a) V. V. Filichev, E. B. Pedersen, *Wiley Encycl. Chem. Biol.* **2009**, *1*, 493–524; b) R. Varghese, H. A. Wagenknecht, *Chem. Commun.* **2009**, 2615–2624; c) H. A. Wagenknecht, *Angew. Chem.* **2009**, *121*, 2878–2881; *Angew. Chem. Int. Ed.* **2009**, *48*, 2838–2841; d) V. L. Malinovskii, D. Wenger, R. Haner, *Chem. Soc. Rev.* **2010**, *39*, 410–422.
- [2] a) W. M. Campbell, K. W. Jolley, P. Wagner, K. Wagner, P. J. Walsh, K. C. Gordon, L. Schmidt-Mende, M. K. Nazeeruddin, Q. Wang, M. Gratzel, D. L. Officer, *J. Phys. Chem. C* **2007**, *111*, 11760–11762; b) W. M. Campbell, A. K. Burrell, D. L. Officer, K. W. Jolley, *Coord. Chem. Rev.* **2004**, *248*, 1363–1379.
- [3] L. M. Moreira, F. V. dos Santos, J. P. Lyon, M. Maftoum-Costa, C. Pacheco-Soares, N. S. da Silva, *Aust. J. Chem.* **2008**, *61*, 741–754.
- [4] I. Bouamaied, L. A. Fendt, D. Haussinger, M. Wiesner, S. Thoni, N. Amiot, E. Stulz, *Nucleosides Nucleotides Nucleic Acids* **2007**, *26*, 1533–1538.
- [5] L. A. Fendt, I. Bouamaied, S. Thoni, N. Amiot, E. Stulz, *J. Am. Chem. Soc.* **2007**, *129*, 15319–15329.
- [6] I. Bouamaied, T. Nguyen, T. Ruhl, E. Stulz, *Org. Biomol. Chem.* **2008**, *6*, 3888–3891.
- [7] T. Nguyen, A. Brewer, E. Stulz, *Angew. Chem.* **2009**, *121*, 2008–2011; *Angew. Chem. Int. Ed.* **2009**, *48*, 1974–1977.
- [8] M. Endo, M. Fujitsuka, T. Majima, *Tetrahedron* **2008**, *64*, 1839–1846.
- [9] a) K. Borjesson, J. Tumpane, T. Ljungdahl, L. M. Wilhelmsson, B. Norden, T. Brown, J. Martensson, B. Albinsson, *J. Am. Chem. Soc.* **2009**, *131*, 2831–2839; b) K. Borjesson, J. Wiberg, A. H. El-Sagheer, T. Ljungdahl, J. Martensson, T. Brown, B. Norden, B. Albinsson, *ACS Nano* **2010**, *4*, 5037–5046.
- [10] H. Morales-Rojas, E. T. Kool, *Org. Lett.* **2002**, *4*, 4377–4380.
- [11] S. Sitaula, S. M. Reed, *Bioorg. Med. Chem. Lett.* **2008**, *18*, 850–855.
- [12] M. Balaz, A. E. Holmes, M. Benedetti, G. Proni, N. Berova, *Bioorg. Med. Chem.* **2005**, *13*, 2413–2421.
- [13] M. Balaz, K. Bitsch-Jensen, A. Mamma, G. A. Ellestad, K. Nakanishi, N. Berova, *Pure Appl. Chem.* **2007**, *79*, 801–809.
- [14] A. Mamma, T. Asakawa, K. Bitsch-Jensen, A. Wolfe, S. Chaturantabut, Y. Otani, X. X. Li, Z. M. Li, K. Nakanishi, M. Balaz, G. A. Ellestad, N. Berova, *Bioorg. Med. Chem.* **2008**, *16*, 6544–6551.
- [15] M. Balaz, A. E. Holmes, M. Benedetti, P. C. Rodriguez, N. Berova, K. Nakanishi, G. Proni, *J. Am. Chem. Soc.* **2005**, *127*, 4172–4173.
- [16] a) M. Balaz, B. C. Li, S. Jockusch, G. A. Ellestad, N. Berova, *Angew. Chem.* **2006**, *118*, 3610–3613; *Angew. Chem. Int. Ed.* **2006**, *45*, 3530–3533; b) M. Balaz, B. C. Li, J. D. Steinkruger, G. A. Ellestad, K. Nakanishi, N. Berova, *Org. Biomol. Chem.* **2006**, *4*, 1865–1867; c) M. Balaz, J. D. Steinkruger, G. A. Ellestad, N. Berova, *Org. Lett.* **2005**, *7*, 5613–5616.
- [17] M. Endo, M. Fujitsuka, T. Majima, *J. Org. Chem.* **2008**, *73*, 1106–1112.
- [18] K. Berlin, R. K. Jain, M. D. Simon, C. Richert, *J. Org. Chem.* **1998**, *63*, 1527–1535.
- [19] A. Onoda, M. Igarashi, S. Naganawa, K. Sasaki, S. Ariyasu, T. Yamamura, *Bull. Chem. Soc. Jpn.* **2009**, *82*, 1280–1286.
- [20] H. D. Li, O. S. Fedorova, W. R. Trumble, T. R. Fletcher, L. Czuchajowski, *Bioconjugate Chem.* **1997**, *8*, 49–56.
- [21] A. Mamma, G. Pescitelli, T. Asakawa, S. Jockusch, A. G. Petrovic, R. R. Monaco, R. Purrello, N. J. Turro, K. Nakanishi, G. A. Ellestad, M. Balaz, N. Berova, *Chem. Eur. J.* **2009**, *15*, 11853–11866.
- [22] A. W. I. Stephenson, N. Bomholt, A. Partridge, V. V. Filichev, *ChemBioChem* **2010**, *11*, 1833–1839.
- [23] a) V. V. Rostovtsev, L. G. Green, V. V. Fokin, K. B. Sharpless, *Angew. Chem.* **2002**, *114*, 2708–2711; *Angew. Chem. Int. Ed.* **2002**,

- 41, 2596–2599; b) C. W. Tornøe, C. Christensen, M. Meldal, *J. Org. Chem.* **2002**, *67*, 3057–3064.
- [24] S. H. Weisbrod, A. Marx, *Chem. Commun.* **2008**, 5675–5685.
- [25] a) A. H. El-Sagheer, T. Brown, *Chem. Soc. Rev.* **2010**, *39*, 1388–1405; b) P. M. E. Gramlich, C. T. Wirges, A. Manetto, T. Carell, *Angew. Chem.* **2008**, *120*, 8478–8487; *Angew. Chem. Int. Ed.* **2008**, *47*, 8350–8358.
- [26] D. Graham, J. A. Parkinson, T. Brown, *J. Chem. Soc. Perkin Trans. I* **1998**, 1131–1138.
- [27] M. Grotli, M. Douglas, R. Eritja, B. S. Sproat, *Tetrahedron* **1998**, *54*, 5899–5914.
- [28] I. Géci, V. V. Filichev, E. B. Pedersen, *Bioconjugate Chem.* **2006**, *17*, 950–957.
- [29] M. Nath, J. C. Huffman, J. M. Zaleski, *J. Am. Chem. Soc.* **2003**, *125*, 11484–11485.
- [30] E. Schwartz, S. Le Gac, J. Cornelissen, R. J. M. Nolte, A. E. Rowan, *Chem. Soc. Rev.* **2010**, *39*, 1576–1599.
- [31] E. E. Bonfantini, A. K. Burrell, W. M. Campbell, M. J. Crossley, J. J. Gosper, M. M. Harding, D. L. Officer, D. C. W. Reid, *J. Porphyrins Phthalocyanines* **2002**, *6*, 708–719.
- [32] H. Firouzabadi, N. Iranpoor, S. Sobhani, *Tetrahedron* **2004**, *60*, 203–210.
- [33] A. W. I. Stephenson, P. Wagner, A. C. Partridge, K. W. Jolley, V. V. Filichev, D. L. Officer, *Tetrahedron Lett.* **2008**, *49*, 5632–5635.
- [34] E. E. Bonfantini, D. L. Officer, *Tetrahedron Lett.* **1993**, *34*, 8531–8534.
- [35] M. Séverac, L. Le Pleux, A. Scarpaci, E. Blart, F. Odobel, *Tetrahedron Lett.* **2007**, *48*, 6518–6522.
- [36] D. M. Shen, C. Liu, Q. Y. Chen, *Eur. J. Org. Chem.* **2007**, 1419–1422.
- [37] J. M. Barbe, G. Canard, S. Brandes, R. Guillard, *Eur. J. Org. Chem.* **2005**, 4601–4611.
- [38] a) A. E. Beilstein, M. W. Grinstaff, *Chem. Commun.* **2000**, 509–510; b) S. I. Khan, M. W. Grinstaff, *J. Am. Chem. Soc.* **1999**, *121*, 4704–4705.
- [39] a) M. Rist, N. Amann, H. A. Wagenknecht, *Eur. J. Org. Chem.* **2003**, 2498–2504; b) E. Mayer, L. Valis, C. Wagner, M. Rist, N. Amann, H. A. Wagenknecht, *ChemBioChem* **2004**, *5*, 865–868.
- [40] a) V. V. Filichev, E. B. Pedersen, *J. Am. Chem. Soc.* **2005**, *127*, 14849–14858; b) V. V. Filichev, I. V. Astakhova, A. D. Malakhov, V. A. Korshun, E. B. Pedersen, *Chem. Eur. J.* **2008**, *14*, 9968–9980.
- [41] V. Hong, S. I. Presolski, C. Ma, M. G. Finn, *Angew. Chem.* **2009**, *121*, 10063–10067; *Angew. Chem. Int. Ed.* **2009**, *48*, 9879–9883.
- [42] D. Globisch, N. Bomholt, V. V. Filichev, E. B. Pedersen, *Helv. Chim. Acta* **2008**, *91*, 805–818.
- [43] R. L. Weller, S. R. Rajski, *Org. Lett.* **2005**, *7*, 2141–2144.
- [44] I. Géci, V. V. Filichev, E. B. Pedersen, *Chem. Eur. J.* **2007**, *13*, 6379–6386.
- [45] C. Bouillon, A. Meyer, S. Vidal, A. Jochum, Y. Chevolot, J. P. Cloarec, J. P. Praly, J. J. Vasseur, F. Morvan, *J. Org. Chem.* **2006**, *71*, 4700–4702.
- [46] J. Kyrp, I. Kejnovska, D. Renciuik, M. Vorlickova, *Nucleic Acids Res.* **2009**, *37*, 1713–1725.
- [47] a) G. Manzini, N. Yathindra, L. E. Xodo, *Nucleic Acids Res.* **1994**, *22*, 4634–4640; b) V. Mathur, A. Verma, S. Maiti, S. Chowdhury, *Biochem. Biophys. Res. Commun.* **2004**, *320*, 1220–1227.
- [48] a) K. Gehring, J. L. Leroy, M. Gueron, *Nature* **1993**, *363*, 561–565; b) J. L. Leroy, K. Gehring, A. Kettani, M. Gueron, *Biochemistry* **1993**, *32*, 6019–6031.
- [49] J. L. Mergny, L. Lacroix, X. G. Han, J. L. Leroy, C. Helene, *J. Am. Chem. Soc.* **1995**, *117*, 8887–8898.
- [50] a) MacroModel, version 9.8, Schrodinger, LLC, New York, NY, **2010**. b) S. J. Weiner, P. A. Kollman, D. T. Nguyen, D. A. Case, *J. Comput. Chem.* **1986**, *7*, 230–252; c) S. J. Weiner, P. A. Kollman, D. A. Case, U. C. Singh, C. Ghio, G. Alagona, S. Profeta, P. Weiner, *J. Am. Chem. Soc.* **1984**, *106*, 765–784.
- [51] G. Manzini, L. E. Xodo, D. Gasparotto, F. Quadrifoglio, G. A. Vandermarel, J. H. Vanboom, *J. Mol. Biol.* **1990**, *213*, 833–843.
- [52] W. C. Still, A. Tempeyk, R. C. Hawley, T. Hendrickson, *J. Am. Chem. Soc.* **1990**, *112*, 6127–6129.
- [53] Insight II, version 9.72, Accelrys Inc., San Diego, CA, **2005**.

Received: November 8, 2010

Revised: February 1, 2011

Published online: April 18, 2011